Evaluation of indoor environment and energy performance of dwellings in heritage buildings. The case of hot summers in historic cities in Mediterranean Europe.

Abstract

The potential benefits for making the historic buildings of heritage cities non-polluting and energy efficient have only recently stirred the interest of researchers and policy makers in facing the necessary challenges. In southern Europe, most of these buildings are residential and are mainly listed at low grades of protection, allowing for significant transformation.

This article quantitatively evaluates the indoor environment and energy performance of the residential heritage building stock under the severe summer conditions characteristic of the Mediterranean climate zone. The historic centre of Seville (Andalusia, Spain) is used as a case study. Three dwellings located in representative listed buildings within its conservation area were monitored and analysed taking occupant behaviour into account. The findings show that many dwellings may lack thermal comfort conditions, which cannot always be guaranteed by passive strategies alone. In addition, these buildings are more polluting than recently constructed ones because they depend entirely for their energy supply on the public electricity grid. Interestingly, in most cases reducing the mechanical cooling demand would not require intrusive physical interventions, but would largely rely on suitable window shading and nightly natural ventilation when outdoor conditions allow.

Keywords: Mediterranean city; city decarbonisation; historic city; architectural heritage; residential heritage; historic buildings; thermal comfort; occupant behaviour; energy efficiency; energy retrofit.

Abbreviations

BEM: building energy model

CTE-HE: Spanish energy code

IRH: Indoor relative humidity (%)

IAQ: Indoor air quality

IAT: Indoor air temperature (ºC)

MM: Mixed Mode adaptive thermal comfort model for hybrid buildings

NNVC: Natural night ventilation cycle

NNVE: Natural night ventilation effectiveness

OAT: Outdoor air temperature (ºC)

ORH: Outdoor relative humidity (%)

TSC: Thermal stability coefficient

T_{op}: Optimal indoor operative temperature (ºC)

T_o: Outdoor reference temperature (ºC)

Table of contents

1. Introduction

According to recent findings from the UN [1] further action is needed to meet energy goals by 2030, and efficiency efforts must focus on the limited overall progress on renewable energy and the increasing energy intensity of the residential building sector. One of the major challenges lies in historic buildings and cities where energy retrofits - despite their considerable potential for reducing energy use – are still perceived as a cultural risk since the conservation principles regulating their treatment might interfere with the renovation plans [2]. This explains why most European countries chose to waive energy efficiency measures in officially protected buildings, as permitted in Article 5 of Directive 2012/27/EU on energy efficiency.

Nevertheless, in recent years an increasing number of researchers and policy-makers, motivated by a new sustainability-centred heritage conservation approach in line with the current 'UNESCO Recommendation on the Historic Urban Landscape [3]' and The Valletta Principles [4], have started to perceive the exclusion of historic building stocks from the urban decarbonisation procedures as a risk which would condemn these historic districts 'to comfort obsolescence or to energy wasting' [5] and jeopardize their healthy survival. Accordingly, major EU research programs on urban heritage rehabilitation were launched between 2013 and 2016 [6]–[8] generating an increase in the literature [9], [10]. The balance between energy consumption reduction and conservation principles was the dominant criterion in this period of growth [2], due to a pressing need to conserve the physical integrity of historic buildings. As a result this field of research continues to focus excessively on construction materials and technical measures, relating exclusively to the buildings themselves, despite the different energy-efficiency-related parameters linked to socioeconomic aspects, and the fact that in the last decade the scientific community has identified user-driven energy parameters in buildings as critical [11]–[13]. Consequently, important urban and indoor environment aspects are frequently forgone, flooding this field of research with open questions, many of which have inspired this study.

The main objective of this investigation is to assess the indoor environmental quality, thermal comfort and energy performance of dwellings within listed buildings of Mediterranean historic town centres under summer conditions, considering human behaviour as a main factor. The city of Seville (Andalusia, Spain) was chosen as a case study, monitoring and analysing three real dwellings in representative protected buildings within its conservation area. Seville is one of the richest EU cities in terms of building heritage and its summer climate is extremely hot and dry, with high solar radiation and outdoor temperatures. Indoor thermal comfort in historic buildings in Mediterranean climate cities has traditionally been reliant on passive energy strategies closely linked to human behaviour. However, their potential should not be overestimated, as natural ventilation, one of the key user-driven passive strategies during summer in southern Europe, cannot always be guaranteed in its historic districts, 'due to high levels of noise, concerns about security, pollution and high night temperatures' [14]. In addition, population growth and housing shortage in the historic city centres at specific points caused irreversible morphological and constructive transformations of the houses directly impacting their energy performance.

Unlike other Mediterranean areas in similar socio-cultural contexts [15]–[18] and despite the wealth of Spanish heritage housing, strikingly little attention has been dedicated to the issue, and specific studies [19], focused on the residential stock, have only recently emerged in the literature. In contrast, energy performance and thermal comfort in social housing in Mediterranean regions have been extensively researched [20]–[25], although conclusions cannot be extrapolated to non-social housing stock under different socio-economic conditions. Therefore, further case studies are needed to obtain reliable empirical data on historic housing, taking different characteristics into account. The data and analysis presented here will contribute to addressing this need and to designing comprehensive retrofit strategies avoiding the potential risks for the conservation of residential urban heritage.

2. Materials and Methods.

This work methodology can be generally applied to the evaluation of energy performance and indoor environment of buildings. It has been employed in previous research on social housing in the same climate zone and with the same general aim [22], [23], [26], [27]. Since this work targets common residential historic buildings in Seville, without exceptional geometrical or constructive features, the methodology can be confidently applied. It consists of four stages: monitoring, user pattern analysis, indoor environmental assessment and energy simulation.

2.1. Monitoring

Five physical parameters related to the energy performance of buildings were monitored during summer 2017: indoor CO_2 air concentration, indoor air temperature (IAT), outdoor air temperature (OAT) and indoor and outdoor relative humidity (IRH, ORH). In addition, airtightness tests of the envelope were also carried out for each case study given its substantial influence on hygrothermal performance, energy consumption and indoor air quality of buildings [28], [29]. The Blower Door Test, the most widely-accepted method in the scientific community for evaluating airtightness in buildings, was used to develop depressurization and pressurization tests following UNE EN-13829 [30], and the equipment was fitted to the entrance door of each dwelling and controlled from the inside. The climate data obtained from two AEMET [31] meteorological stations located in Seville was compared to several one-off OAT measurements captured next to the buildings of the case studies. Hourly average values of IAT in degrees centigrade (ºC), indoor CO_2 air concentration in parts per million (ppm) and indoor air RH in percentage (%) were recorded for a one-month period in summer 2017 using WOHLER CDL 210 indoor data-loggers recording at 30-minute intervals, and using the data from the living room and bedroom of individual dwellings. The accuracy of the data provided is ±5% for CO_2 concentration and relative humidity and ±0.6ºC for temperature measurements. Technical characteristics of the air-conditioning systems and appliances (type, make and model, input electrical

power, efficiency coefficient EER and COP, etc…) and energy bills for 2017 and the two years preceding were also compiled for each case study.

2.2. User pattern analysis

As some major differences between the expected and the measured energy performance of buildings were shown to be the result of mistaken assumptions regarding occupant behaviour [13], qualitative data were collected through surveys and personal interviews and afterwards compared to quantitative data for validation. The surveys and interviews, conducted at the dwellings at several points of the monitoring campaign, focused on occupancy (density and duration), natural ventilation habits (when and for how long each room is ventilated) and cooling (kind of system or systems used, when they are commonly switched on and for how long. Residents' daily routines (use of rooms, usual set-point temperature of the cooling system, cooking habits…) and personal preferences relating to thermal comfort, including the preferred level of clothing indoors, were also recorded. The outcomes are described in full in **Section *3.3.3*.**

Indoor CO_2 concentration rates were used to establish occupancy hours and - in combination with OAT, IAT and RH rates - to deduce the natural ventilation periods. Sharp changes in IAT were used to infer cooling system operation. When extended periods of natural ventilation were declared, as in Case 3, the indoor CO_2 concentration levels were not used to deduce presence, and the occupancy schedule stated in the survey was adopted. Daily routines were examined over a typical period of 11 days, including weekdays and weekends, extracted from the monthly measurements collected (**Fig. 12**, **Fig. 13**). Two sample days were chosen from each case study for more in-depth descriptions of hourly practices in occupancy, natural ventilation and cooling operation (**Fig. 14**, **Fig. 15**, **Fig. 16**).

2.3. Indoor environmental analysis

Indoor environment evaluation was based on measured data and included: indoor CO_2 concentration, IRH, and thermal comfort. Additional parameters were also considered:

- Thermal Stability Coefficient (TSC), which measures the relationship between indoor and outdoor amplitude temperature. Values around 1 indicate that the space has a low thermal inertia, with any energy changes (indoor or outdoor) thus becoming immediately apparent in the indoor environment, while values below 0.5 show high thermal inertia in the room, taking more time or energy to change indoor temperature [32]. TSC values were obtained for periods in which the dwellings were unoccupied, in order to compare their thermal inertia.
- Natural night ventilation effectiveness (NNVE), which measures the speed of reduction in IAT (in ºC per hour) during ventilation cycles.

CO_2 concentration is the main source of air pollution in residential buildings. The upper threshold adopted, below which IAQ is considered good, was 1200 ppm [33]. Given the links between excessive levels of IRH and adverse health effects and building pathologies, design values between 20-70% are advised in European standard EN15251 [34] for the less demanding Category III of existing buildings.

Two indexes were used for the thermal comfort evaluation:

- Average deviation of the measured IATs in relation to the daily optimal indoor operative temperature (T_{op}) in degrees Celsius.
- Percentage of occupied hours of discomfort (%).

The results were compared to the percentage of hours of use of the cooling system.

Since the monitoring findings on the case studies showed intermittent use by occupants of the mechanical cooling system, adaptive thermal comfort models were found to be more appropriate for application in this research than the steady-state based models. Adaptive comfort theory considers that

T_{op} for occupants who can interact with the building and its devices relates primarily to the outdoor environmental conditions, a relationship expressed by the following linear equation [35]:

$$\boldsymbol{T_{op} = a \cdot T_o + b} \quad (1)$$

where: *a* is the slope of the function, proportional to the degree of adaptation to regional climatic conditions; T_o is the outdoor reference temperature and *b* is the y-intercepted. Both *a* and *b* are statistically fitted to data collected from field studies.

Three adaptive thermal comfort standards were used to calculate optimal, upper and lower limit values of T_{op}: Standard 55 from ASHRAE (for naturally ventilated, non-mechanically-cooled buildings) [36], prEN 16798-1 from CEN (for spaces with no established strict dressing protocols and operable windows, or when a non-mechanical cooling system is in operation) [37] and the more recently developed MM model [38] suited to the same climate zone. Neither of the first two exactly addresses the cooling operation profile of these cases studies. In contrast, the third, proposed as an alternative model for Mediterranean climate and for buildings with predominant hybrid operation, is best suited to our case. According to the authors 'Hybrid or mixed mode (MM) buildings refer to a space conditioning approach that combines natural conditioning (through windows with mechanical or controlled opening mechanisms) and mechanical conditioning, allowing a change from one mode to another, when necessary'.

As the heritage assets of the case study buildings may restrict retrofit measures, the three standards were applied under low-demand acceptability ranges: Standard 55 under the range of 80% satisfied occupants, with a temperature interval of ± 3.5ºC; EN 16798-1 under building category III, for a moderate level of expectation and with a temperature interval of ± 4ºC; and MM model under the range of 85% satisfied occupants, with a temperature interval of ± 3.5ºC. The outdoor reference temperature (T_o) applicable range is 10ºC ≤ T_o ≤ 33.5ºC for Standard 55; and 10ºC ≤ T_o ≤ 30ºC for EN 16798-1

and MM models. The linear relationship, represented by a general equation (1), between T_{op} and T_o for each day of a particular year is specific to each adaptive model:

$$\boldsymbol{T_{op} = 0.33 \cdot T_o + 18.8} \quad (2)$$

suited to EN 16798-1;

$$\boldsymbol{T_{op} = 0.31 \cdot T_o + 17.8} \quad (3)$$

to Standard 55; and

$$\boldsymbol{T_{op} = 0.24 \cdot T_o + 19.3} \quad (4)$$

to the MM model.

After calculating T_o according to the standards, the three comfort bands were obtained for each day of July-August 2017 and represented in a graph (**Fig. 1**) revealing that while T_{op} lower limits are similar in the three models, prEN 16798-1, the least restrictive, allows a significant increase in the upper limit in relation to Standard 55 and to the MM model (2ºC and 2.5ºC on average respectively), causing major divergences in the percentage of hours of discomfort, as described in **Section *4.1.2***

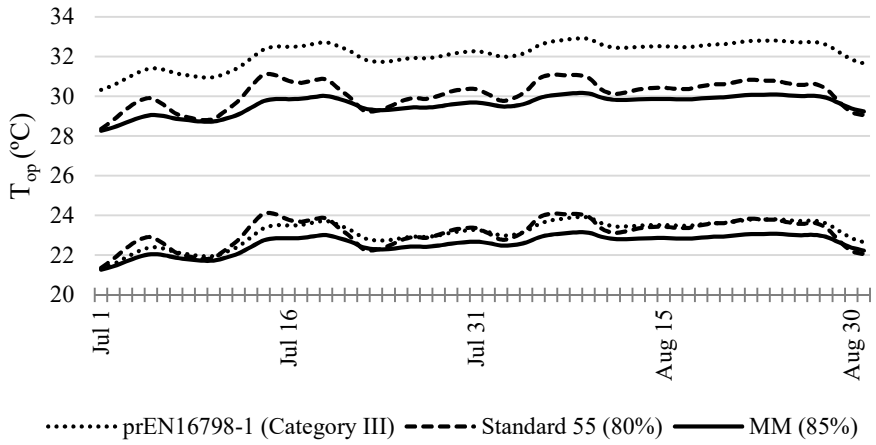

Fig. 1. Comfort bands for July and August 2017, where upper and lower limits of T_{op} are set following prEN 16798-1, Standard 55 and MM adaptive thermal comfort models. In order to determine the proportion of occupied hours

of discomfort, two user profiles were considered: (1) the standard profile established by CTE-HE (24h profile) [39], which considers a positive sensible load throughout the day in all the rooms, and (2) an alternative night-day profile [22] adjusted to the user pattern inferred from the monitoring data collection, which considers a day-time occupancy for the living room (8-23h, with no occupancy in the bedroom) and night-time occupancy for the bedroom (24-7h, with no occupancy in the living room), with no distinction between weekdays and weekends.

2.4. Energy simulation

The energy model for each case study was initially constructed using the input data obtained from the climate data, envelope characterization audit, air tightness tests, user pattern examination and an indoor environmental analysis described in **Sections 3** and **4.1.1.** The energy model was then calibrated using the IAT data.

Building energy models (BEMs) provide hourly calculations of key indoor environmental parameters. Discrepancies are commonly identified between the simulated and measured outputs, due to the random behaviour of building users and the lack of control of the pathologies generated in the construction or operation of the buildings [40]. In order to reduce their uncertainty, so that they may be confidently used as a predictive tool, BEMs must be calibrated. The calibration process can be done manually, in an iterative process of adjusting model inputs and recomposing the results to measured data, or by using systematic and automated procedures, as there is not yet a commonly accepted methodology [40], [41]. Energy consumption is the parameter generally used to calibrate the BEMs, though IAT is more suitable for buildings without mechanical cooling and/or heating or cases where these systems are used sporadically. The statistical quantification of the error is executed after a calibration process. A BEM is considered in calibration when the statistical indices demonstrating calibration have been met [42].

2.4.1. Energy model construction

The energy model was constructed with Design Builder (v.4.7.0.027) software which uses Energy Plus [43], a calculation engine recognized by the US DOE [44]. The climate data used was provided by two Meteorological Stations located in Seville and belonging to AEMET, the Spanish State Meteorological Agency [31]. All the information gathered and analysed following the above method was introduced in the model.

2.4.2. Energy model calibration

IAT simulated and measured rates for the typical week were first compared graphically (**Section *4.2.1.*** and iteratively adjusted. The results of this manual calibration were statistically validated following 2015 U.S. Department of Energy M&V Guidelines [45] which use the indices of Mean Bias Error (MBE) and Coefficient of variation of the Root Mean Square Error (CvRMSE) to represent how well a mathematical model describes the variability in measured data.

$$\text{MBE (\%)} = \frac{\sum_{i=1}^{Ni}(Mi-Si)}{\sum_{i=1}^{Ni} Mi} \times 100 \quad (5)$$

$$\text{CvRMSE (\%)} = \frac{RMSE}{\frac{1}{Ni}\sum_{i=1}^{Ni} Mi} \times 100 \quad (6)$$

$$\text{RMSE} = \sqrt{\sum_{i=1}^{Ni} \frac{(Mi-S\ )^2}{Ni}} \quad (7)$$

where: Mi is the measured data at instance n, Si is the simulated data at instance n, Ni is the number of records used in the calibration and RMSE is the Root Mean Square Error. The model is considered calibrated when MBE hourly values fall within ±10% and CvRMSE falls below 30%.

3. Case studies

3.1. Selection of case studies

As the present study is part of research with a wider scope on decarbonisation of residential heritage at urban scale, the choice of city, its historic neighbourhood and the dwellings within are of prime importance. The large historic city of Seville (Andalusia, Spain), catalogued at regional level as 'Asset of Cultural Interest', the highest protection grade existing in Spain, was chosen for this analysis. It holds 8.2% (57,000) of Seville's total population of 694,000 and since 1990 it has been governed by a Special Protection Plan with binding policies on urban infrastructure, demolitions and building preservation and refurbishment. This area also includes the Cathedral, Alcázar, and Archivo de Indias, which have been included jointly on the World Heritage List since 1987 (**Fig. 2**) [46]. This directly affects the potential urban transformations in a radius of 100 metres (or more if visual integrity is affected). 62% of the buildings within Seville's historic city (6,875 of 11,029) are protected [5].

Two criteria - degree of protection and historic typology - are employed by the local policy on heritage protection to classify this extensive historic building stock. Four grades of protection are stipulated: A and B for monuments, C for buildings of typological interest, and D for buildings which contribute to maintaining urban identity. Buildings listed under grades C and D represent 96% of the total building stock catalogued. This abundance, combined with their great potential for transformation, makes these buildings the most appropriate target for energy retrofit strategies. Regarding historic typologies, eight main categories are established in Seville historic city and three of them, 'Casa de pisos', 'Casa patio' and 'Corral de vecinos', represent 66% of the total listed buildings. The 'Casa de pisos' category is used for multi-family buildings with two or more storeys (usually four) communicated by a common staircase. The ground floor is generally used for commercial premises. The building façade is aligned with the front plot-limit while there is a courtyard at the back for lighting and ventilation. The 'Casa patio' category comprises single-family houses over a quadrangular plot with two or three storeys. The rooms are organized around a large patio in the centre of the plot, and connected by a gallery on the

first floor. A second patio, usually smaller than the first, is located at the back of the plot for ventilation and lighting. The third category, 'Corral de vecinos', is a multi-family building, a specific popular kind of 'Casa patio' where several dwellings are distributed around a common large patio and communicated by galleries. Although these were traditionally two-storeys-high, nowadays most of them have been expanded with a third floor added on top. The square patio provides lighting and ventilation to the individual dwellings.

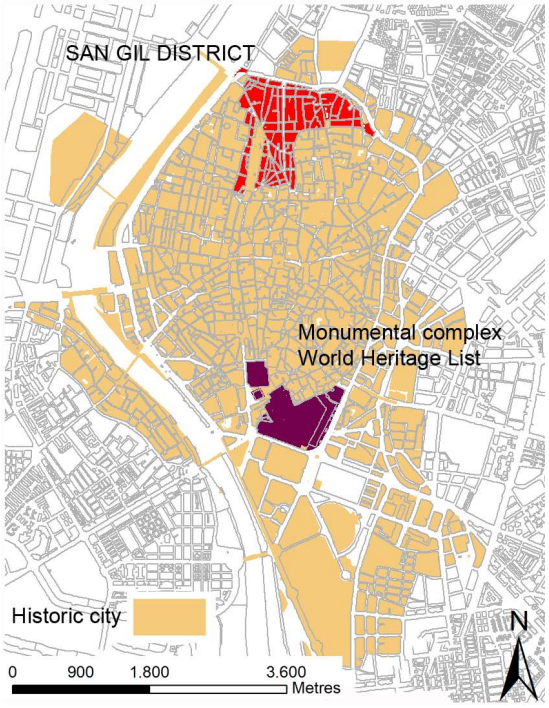

Fig. 2. Map showing the historic city area within the municipality of Seville (brown), the World Heritage Listed complex (purple) and San Gil district (red). Prepared by the authors according to [46],[47].

The most densely populated district within the historic city of Seville is San Gil, with a population of 6,500 people (around 200 inhabitants per hectare). According to the 2015 Census of the city of Seville [47], 16% of the population in the district of San Gil is under 18, 70% between 18-64 and 14% above 64. There are no data on household composition available for San Gil. The vast majority of its buildings (1,221 out of 1,233) are residential. 61% of its total residential buildings are listed (750 of 1,221), mostly under C and D grades (738 of 750), as shown in **Fig. 3**. These characteristics make it the most appropriate urban area for this research. The typological distribution of buildings in San Gil is shown

in **Fig. 4**: 'Casa de pisos' is the most frequent type (308 of 535 residential listed buildings), followed by 'Casa patio' (183 of 535, including the sub-category 'Corral de vecinos').

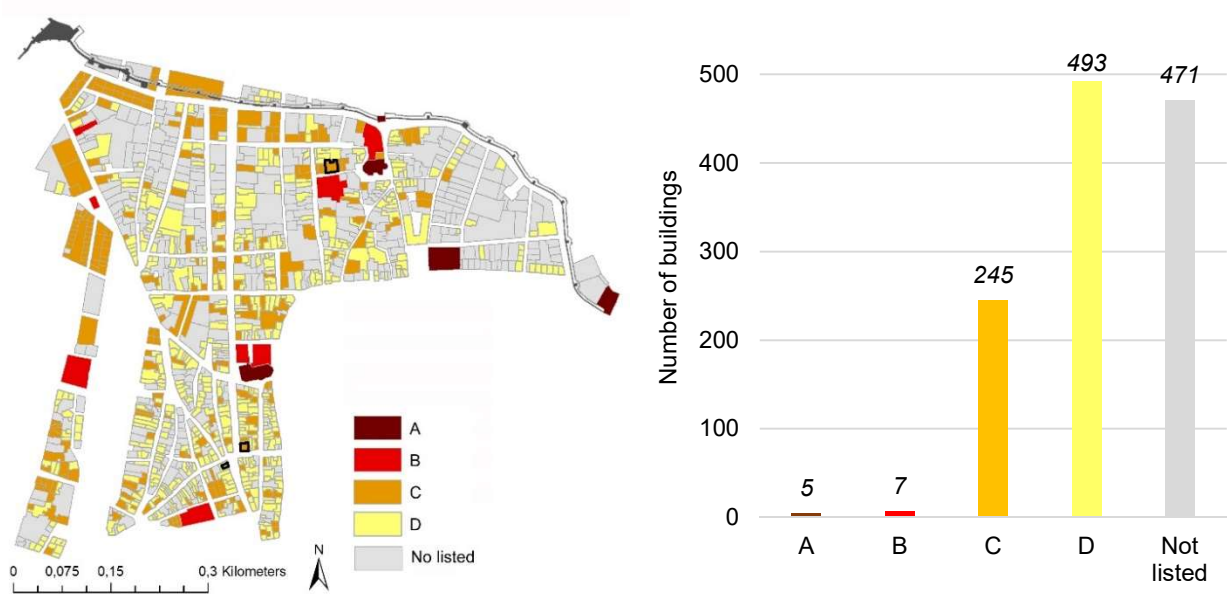

Fig. 3. Classification of the listed buildings in San Gil, Seville, according to the Municipal Catalogue of Protection. On the left, map of San Gil with the four listing grades - A, B, C and D - the highest of which is A. A fifth class of non-listed buildings appears in grey. The three case studies are outlined in black. On the right, bar plot of frequencies for the five types. Prepared by the authors according to the San Gil Special Protection Plan [47].

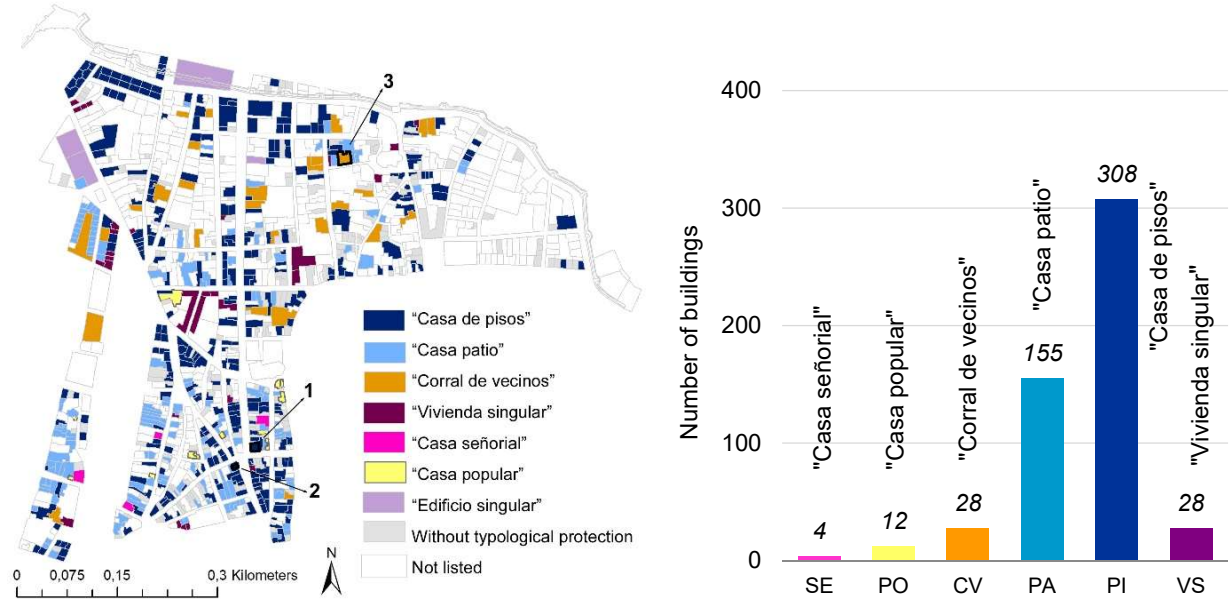

Fig. 4. Typological distribution of category C and D listed buildings in the San Gil district of Seville. On the left, map of San Gil showing the distribution of historic typologies, colour-coded as in the caption. On the right, bar plot of the frequency of building typologies in San Gil. Prepared by the authors according to the San Gil Special Protection Plan [47]

Three apartments in San Gil were selected as case studies on the basis of their typology, grade of protection and demographics, the three criteria used to evaluate the extent to which a building is representative of its residential listed stock. Cases 1 and 2 are 'Casas de pisos' and Case 3 is a 'Corral de vecinos', the two most abundant typologies. All three are catalogued according to the most common grades: Cases 1 and 3 are C-listed and Case 2 is D-listed. Regarding demographics, as Guerra-Santin highlights, two of the main factors which 'can greatly influence the energy requirements in residential buildings are household composition and age, especially in regard to the presence of children and elderly people' [13]. Given the lack of statistical data on household composition in San Gil mentioned above, this demographic factor could not be directly taken into account in the research. However, the population distribution described above can be used to deduce a lower presence of children and elderly people in most of the dwellings in San Gil. Therefore, the residents of the apartments selected are all in the most frequent age category, the 18-64 demographic, while the types of households are also representative, with no children or elderly residents: Cases 1 and 3 are occupied by single individuals in their thirties and Case 2 by a couple aged around forty.

3.2. Climate characteristics.

Seville is located in a Mediterranean climate area, corresponding to the Köppen-Geiger climate classification [48]. Included in zone B4 of the Spanish climatic zoning [39] with the highest value in the scale of summer climate severity, its climate characteristics are summarized in **Table 1** [31], [49].

Table 1
Annual average climate values for Seville (1981-2010)

Latitude: 37° 25' 0" N		Longitude: 5° 52' 45" W		Altitude (m): 34		
Daily temperature (°C)	Max. daily temperature (°C)	Min. daily temperature (°C)	Precipitation (mm)	Relative humidity (%)	Hours of sunlight	Direct solar radiation (kWh/m^2)
19.2	25.4	13	539	59	243	153

During summer 2017, when the monitoring campaign was conducted, 'outdoor temperatures reached 30 ºC for 100% days and on average 46% of the daily hours were above that value. Moreover, in almost

40% of summer days of that period, outdoor temperatures were above 40 ºC, the cut-off point for activating heatwave protocols. Five heatwave periods were recorded in 2017, with minimum outdoor temperatures rarely below 20 ºC and maximum temperatures of up to 47.4 ºC [50]'. The frequent high summer nightly OATs are critical in Seville, as they may make it impossible to cool the dwellings using night natural ventilation. **Fig. 5** shows that from June 15th to September 15th, 2017, 49.4% of the night-time hours (22PM-8AM) OATs were above 26ºC, the recommended upper limit for Category II buildings in European standard prEN15251 [34].

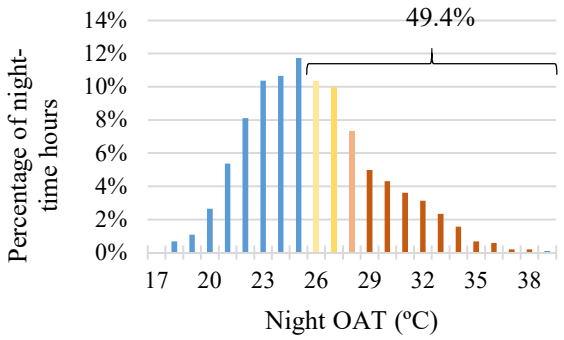

Fig. 5. OAT distribution during night-time hours from June 15th to September 15th 2017. Temperatures below 26 ºC (thermal limit) are represented in blue. Above this limit, they are represented in warm colours.

3.3. Case study description

3.3.1. General features

Case 1 is a first floor apartment located above commercial premises in a six-storey building dating from 1923. It was designed in the characteristic Sevillian regionalist style of the early 20th century by the well-known local architect José Espiau y Muñoz and was first refurbished by his son Ricardo Espiau Suárez de la Viesca in 1967 [51]. Its usable surface of 40.50 m^2 contains a hall, living room, kitchen, bathroom and bedroom. The living room and bedroom are on the main façade, which faces south. The kitchen has access to natural light and ventilation through a window which opens out over a small interior courtyard (**Fig. 6**). The apartment was last renovated in 2004: in addition to the

complete replacement of its facilities, new exterior double-glazing with wooden joinery and interior wooden shutters was fitted on the façade windows. A ducted air-conditioning installation was also installed, with outlets to living room and bedroom in simultaneous operation.

Case 2 is a duplex apartment with an east-facing façade within a 'Casa de pisos' building constructed in 1940. Its second floor is located at the top of the building, with access to a terrace (**Fig. 7**). The dwelling has a usable surface of 64.65 m^2 and was last renovated in 1960 to poor quality standards. The patio was covered with translucent polymethyl methacrylate plates, forming a new space that is vertically closed with a 70 mm sandwich panel. More recently, the large window on the façade was replaced with a double-glazed aluminium one with no thermal break. Neither the gable roof nor the flat terrace roof was thermally insulated. The bedroom monitored, on the first floor, is used both for sleeping (on the hottest summer nights) and working. Since the plot has no inner courtyard, the bedroom has no windows. Natural cross ventilation occurs through a large aluminium sliding window opened on the sandwich panel wall or through the terrace door. The thermal conditioning systems are a heat pump in the living room and portable electric radiators in the rest of the rooms.

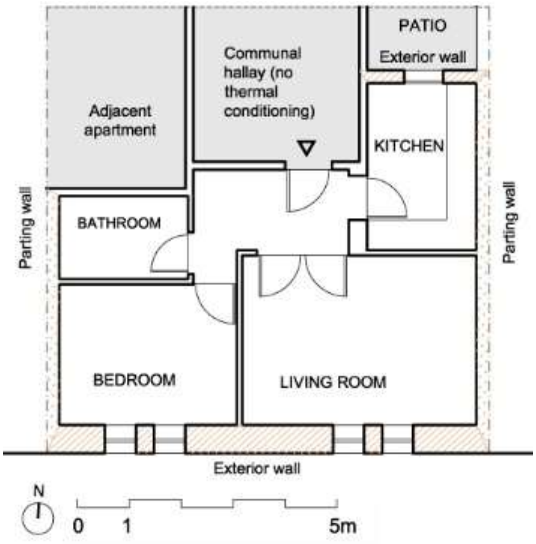

Fig. 6. Floor plan of Case 1 dwelling

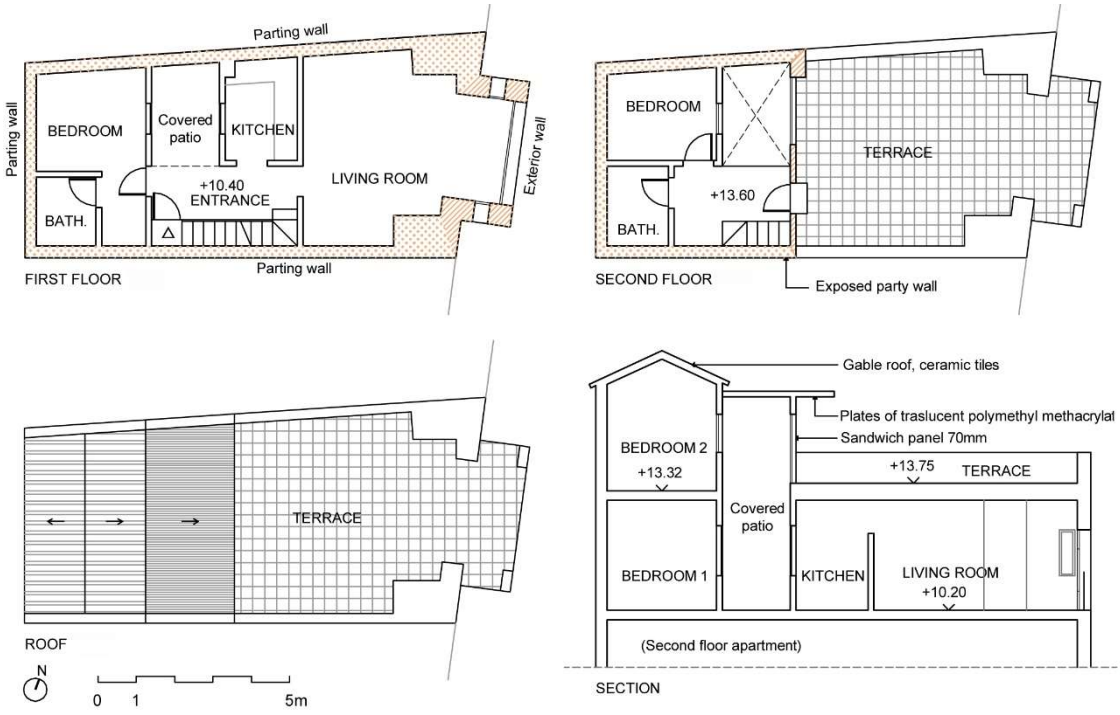

Fig. 7. Floor plans and section of Case 2 dwelling.

Case 3 is a one-floor apartment on the top-floor of a 'Corral de vecinos' building, dating from the late 18th century (**Fig. 8**). The last renovation, in 1992, included the complete replacement of the facilities and new wooden joinery for the façade openings, with single glazing, no thermal break and interior wooden shutters. The flat roof has never been thermally insulated. Case 3 apartment includes living room and kitchen in the same volume, a bedroom and a bathroom in an overall usable surface of 35.20 m^2 (**Fig. 9**). The bathroom is naturally ventilated and lit by a small window which opens onto an inner courtyard. As is usual in southern Spain, the dwelling only has local thermal conditioning systems: a reversible heat pump and an electric heater, both located in the living room.

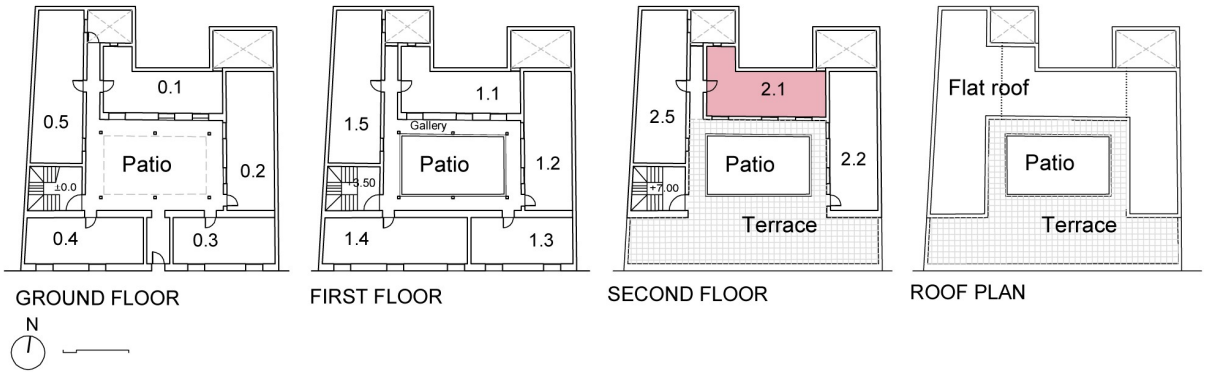

Fig. 8. Case 3: floor plans of the 'Corral de vecinos' building marking the position of the apartment studied in colour.

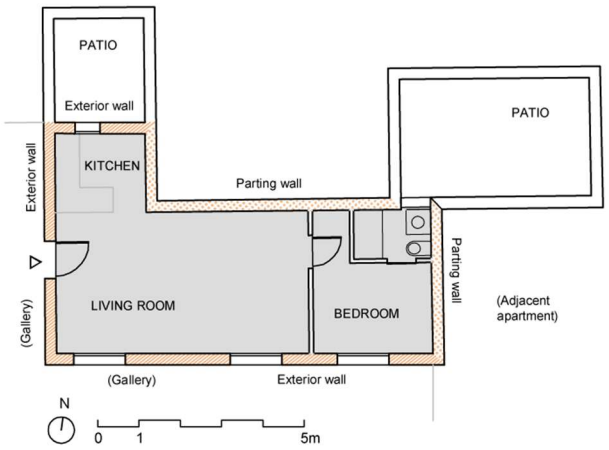

Fig. 9. Case 3. Floor plan.

3.3.2. Envelope characterization.

Envelope characteristics were inferred from in situ inspections and measurements of the main constructive elements (walls, roofs, windows) and compared to the relevant scientific literature on the historic constructive features of Sevillian residential buildings dating from the 18th and 19th centuries [52] and the early 20th century [53]. The outcomes are summarized in **Table 2** and **Table 3**. Air leakage rates, obtained through Blower Door Tests are average for the climate zone [54] for cases 2 and 3 while that for Case 1 is higher. The compactness index, which measures the total volume of the dwelling to its outer surface ratio in m^3/m^2, was also calculated for the three case studies. Exterior views of the three buildings and of the communal patio of Case 3 are shown in **Fig. 10**.

Table 2
Case study envelope thermal characteristics

	Case 1		Case 2		Case 3	
Transmittance, U (W/m^2K)	*Façade*	*Patio*	*Façade*	*Covered patio*	*Façade*	*Patio*
Exterior wall	0.60	1.14	1.56	-	2.26	2.26
Joinery	1.90	5.88	5.88	5.88	1.90	5.88
Glazing	3.23	5.78	3.23	5.78	5.78	5.78
Window	2.96	5.80	3.76	5.80	6.96	5.80
Flat roof	-		3.10		3.10	
Arab tile gable roof	-		2.63		-	
Slabs	2.05		2.05		2.05	
Air leakage rate at 50 Pa: n50(h^{-1})	15.71		7.14		7.71	

Table 3
Case study main features: age, geometry, construction and passive and active cooling systems.

	Case 1	**Case 2**	**Case 3**
Construction date	1923	1940	18th century
Refurbishment dates	1967, 2004	1960	1992
Typology	'Casa de pisos'	'Casa de pisos'	'Corral de vecinos'
Listing grade	C	D	C
Number of storeys of the building	6	4	3
Level position in the building	1	3	3
Main façade solar orientation	South	East	South
Usable floor area (m^2)	40.5	64.65	35.2
Total façade thickness (cm)	55	40	27
Compactness (m^3/m^2)	3.8	3.3	1
Façade composition (outer-inner)	Solid brick facing (24 cm) Air chamber (5 cm) Solid brick (24 cm) Plaster and paint (2cm)	Solid brick facing (24 cm) Air chamber (2 cm) Solid brick (12 cm) Plaster and paint (2cm)	Plaster and paint (2 cm) Solid brick (12 cm) Air chamber (3 cm) Perforated brick (8 cm) Plaster and paint (2 cm)
Type of roof (building)	Rooftop terrace	Rooftop terrace + Arab-tile gable roof	Flat roof
Roof composition (outer-inner)	Tiles (double leaf with mortar) Asphalt sheet Roof structure	Arab tiles Mortar Roof structure	Tiles (double leaf with mortar) Asphalt sheet Roof structure
Joinery (no thermal break)			
Living room, bedroom	Wood (folding)	Aluminium (folding)	Wood (folding)
Kitchen, bathroom	Aluminium (sliding)	Aluminium (sliding)	Aluminium (sliding)
Glazing			
Living room, bedroom	Double clear 3/6/3 mm (air)	Double clear 3/6/3 mm (air)	Single clear 6 mm
Kitchen, bathroom	Single clear 6 mm	Single clear 6 mm	Single clear 6 mm
Window shading	Interior opaque wooden shutters	Interior opaque aluminium shutters	Interior opaque wooden shutters
Ventilation system	Natural through windows, vent in bathroom	Natural through windows, vent in bathrooms	Natural through windows
Hot water production	Electric hot water boiler		
Cooling system	Centralized and ducted installation (living room and bedroom) EER=3.25	Heat pump in living room. EER=2.30	Heat pump in living room. EER=2.60

Fig. 10. Exterior views of Case 1 (a), Case 2 (b) and Case 3 (c). Communal patio of Case 3 (d)

3.3.3. User pattern description

The user profile was defined according to the method described in **Section 2.2.** The information obtained from the surveys regarding occupancy, natural ventilation and cooling system operation, is summarized in **Table 4**. Monthly electricity consumption was averaged from bills for 2017 and the two preceding years (**Fig. 11**a). Based on this, and considering that in all cases energy is entirely provided by the public electricity grid, CO_2 emissions and annual primary energy consumption were calculated and compared to the current CTE-HE upper limits [55] (**Fig. 11**b). Despite the low power consumption, far below the average for Spanish multi-storey buildings in the Mediterranean Climate, which is 6,386.105 kWh per year per dwelling [56], and the low occupancy of the dwellings, and energy obtained entirely from non-renewable sources, the primary energy consumed is 1.80 and 2.75 times above the current limits for Case 1 and 2 respectively, while Case 3, with the lowest power consumption, is almost at the limit. As a result, Cases 1 and 2 would fall within category C and Case 3 would be within category B of CO_2 emissions in the national energy certification system.

Table 4
Surveys on user practices during summer

Case 1		1	2	3	4	5	6	7	8	9	10	11	12	13	14	15	16	17	18	19	20	21	22	23	24
Occupancy	Weekday																								
	Weekend																								
Natural ventilation	Weekday																								
	Weekend																								
Local cooling	Weekday																								
	Weekend																								
Case 2		1	2	3	4	5	6	7	8	9	10	11	12	13	14	15	16	17	18	19	20	21	22	23	24
Occupancy 1	Weekday																								
	Weekend																								
Occupancy 2	Weekday																								
	Weekend																								
Natural ventilation	Weekday																								
	Weekend																								
Local cooling	Weekday																								
	Weekend																								
Case 3		1	2	3	4	5	6	7	8	9	10	11	12	13	14	15	16	17	18	19	20	21	22	23	24
Occupancy	Weekday																								
	Weekend																								
Natural ventilation	Weekday																								
	Weekend																								
Local cooling	Weekday																								
	Weekend																								

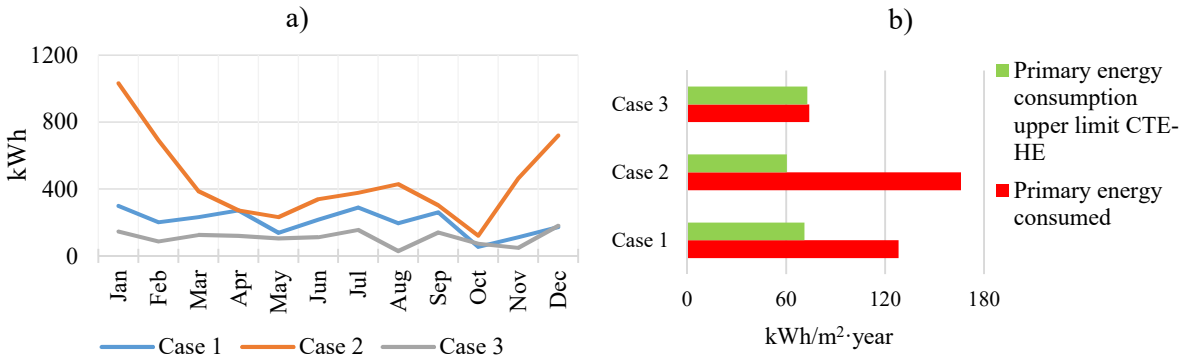

Fig. 11. Comparison of the three case studies: monthly electricity consumption (a) and primary energy annual consumption compared to the current limits (b).

The analysis of hourly IAT evolution, cooling operation and natural ventilation for the typical time period is represented in **Fig. 12**. A sample week was used to describe the cooling profile (**Fig. 13**) and to calibrate the energy model. Daily routines are studied in **Fig. 14**, **Fig. 15** and **Fig. 16**.

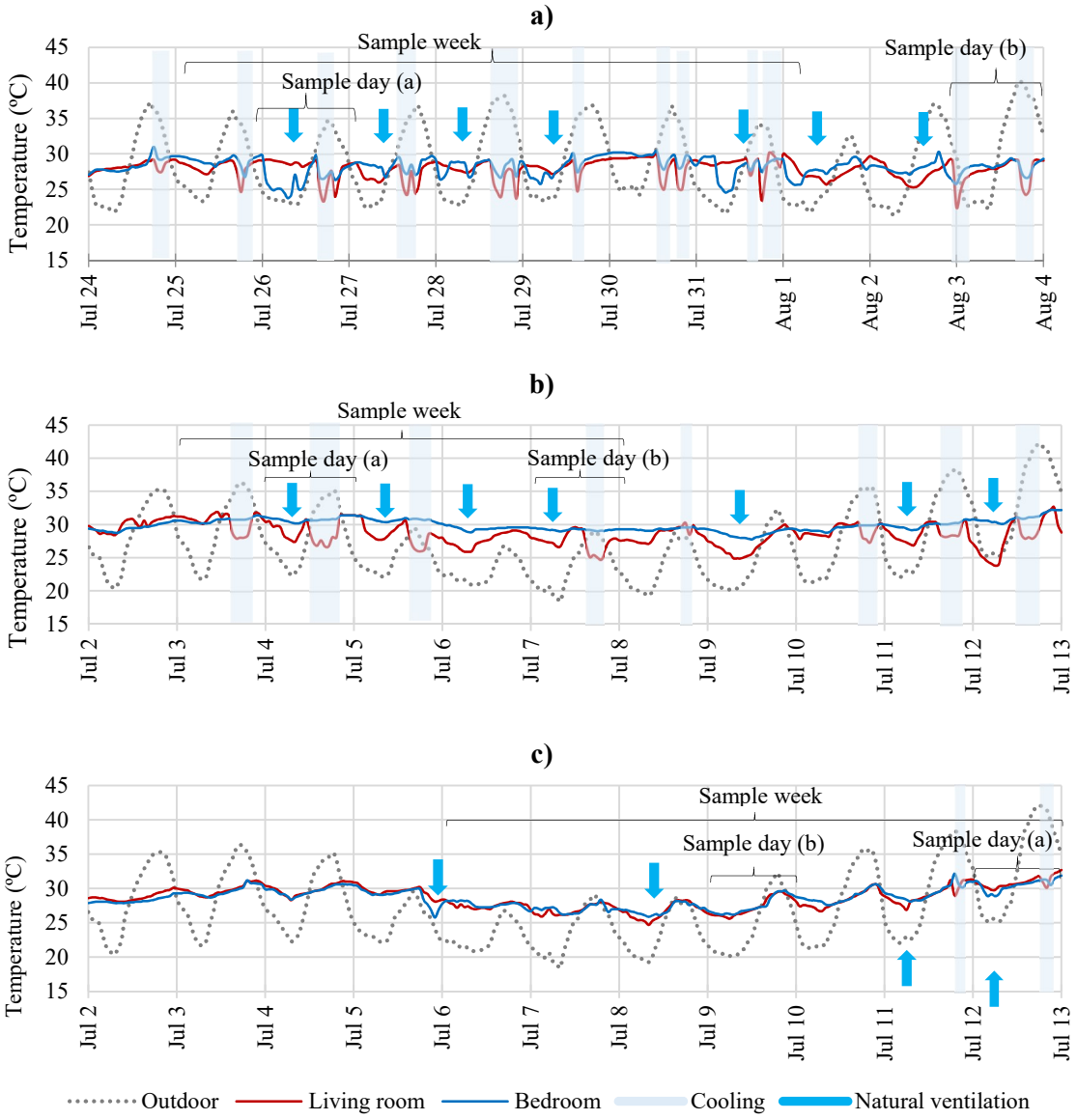

Fig. 12. Hourly temperature evolution in the typical time period, highlighting cooling operation (light blue), natural ventilation (blue arrows) and selection of two sample days to characterize the user pattern and a sample week for energy model calibration: (a) Case 1, (b) Case 2, (c) Case 3. Sample weeks and sample days are bracketed.

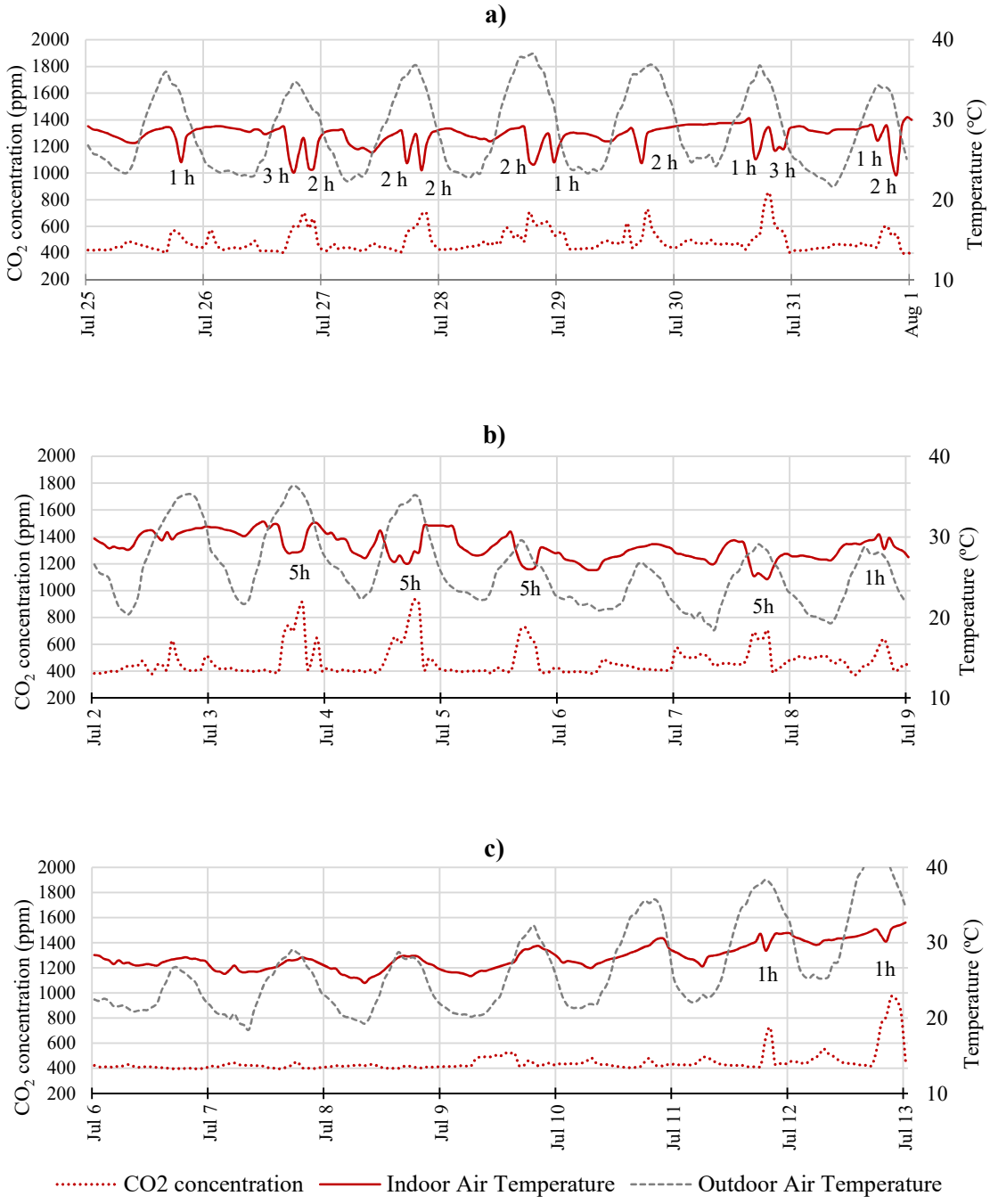

Fig. 13. Cooling operation during the sample week, based on IAT and CO_2 concentration in the living room: (a) Case 1, (b) Case 2, (c) Case 3. Three curves are represented: CO_2 concentration, IAT and OAT. The duration of cooling cycles (in hours) is indicated on the graphs.

Case 1 dwelling is inhabited by a single person who works outside the home on weekday mornings and from home with her computer in the afternoons and evenings. The weekday hours spent at home registered are fewer than those reflected in the survey (27% and 40% respectively). She stated that she

did not open the bedroom window at night because of the street noise, therefore making it easy to establish the nights when the bedroom was occupied through the increase in CO_2 concentration. The cooling was switched on regularly in afternoons and evenings, following an intermittent pattern of no more than 3 hours in a row and set point temperatures of 23-24 ºC predominantly (**Fig. 13**a). Although according to the survey, the percentage of weekday hours of cooling operation is 100% of occupied hours, the percentage registered was 58%. **Fig. 14** shows two typical days: one in which the bedroom was naturally ventilated at night (**Fig. 14a**) and another in which it was not, with one sleeping person (**Fig. 14b**). The annual energy consumption for Case 1 was 2,452 kWh/year. Higher consumption was reached (964 kWh) from June to September.

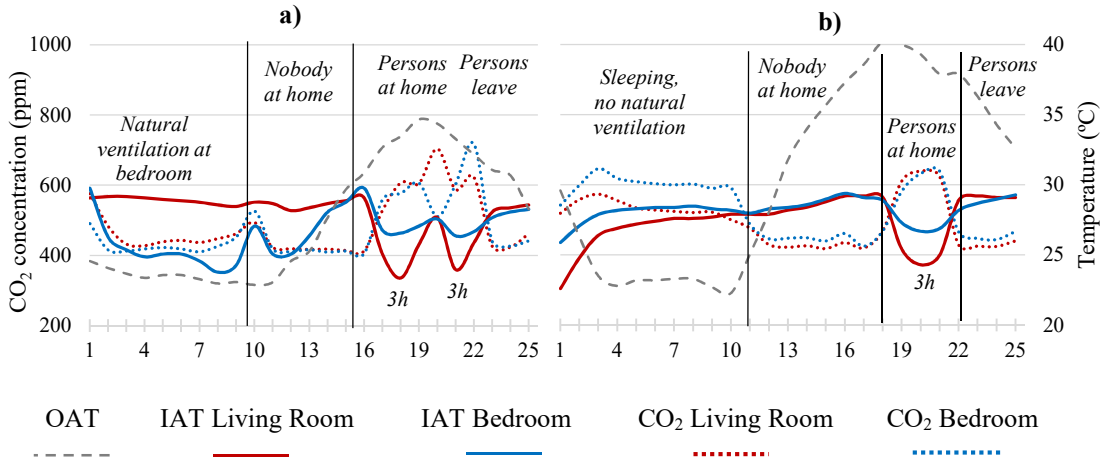

Fig. 14. Case 1. User pattern on two sample days: (a) natural ventilation in the bedroom, (b) one sleeping person without night-time natural ventilation. Cooling cycle duration is marked on the graphs in hours.

Case 2 dwelling is occupied by two professionals, one with a work schedule of 8-21h, while the other works from 8 to 15h. Based on CO_2 recording, the day-time living room occupancy periods are 37% day-time hours, slightly lower than the 47% stated in the survey. The bedroom was occupied on three nights out of eleven, in accordance with the flexible use of this room mentioned in **Section *3.3.1.*** The living room was naturally ventilated almost every night, as recorded in the survey, and the cooling ran steadily for extended periods of 5 or 6 hours in a row (**Fig. 13**b) at a set point temperature ranging from 26 to 28 ºC. According to the survey, the percentage of weekday occupied hours of cooling

operation is 86% but the percentage registered totalled just 66%. Two typical days are shown in: one in which the living room is naturally ventilated at night (**Fig. 15**a) and another in which it is not (**Fig. 15**b). Its annual energy consumption was the highest of the three case studies: 5374.60 kWh/year, including 1452 kWh corresponding to the period from June to September.

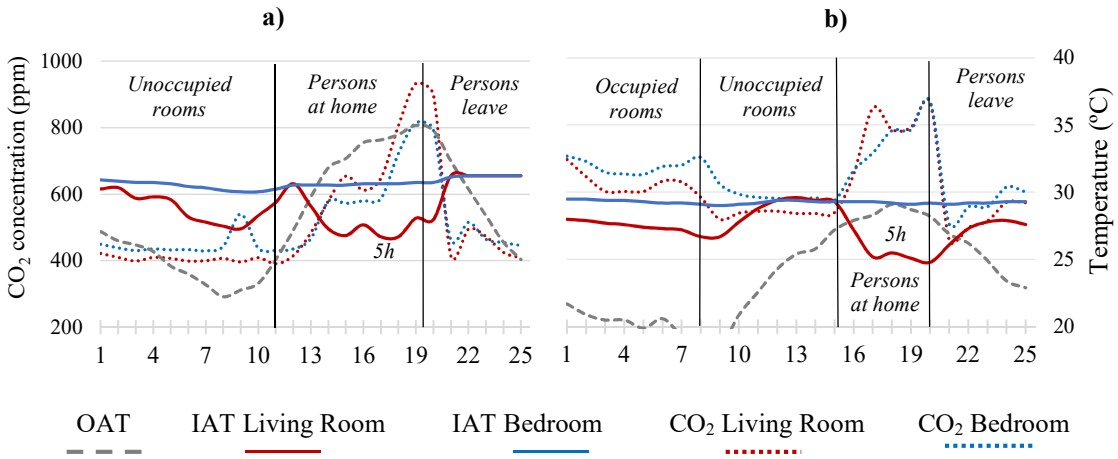

Fig. 15. Case 2. User pattern on two sample days: (a) night natural ventilation in the living room, (b) one sleeping person in the bedroom without night-time natural ventilation. Cooling cycle duration is marked on the graphs in hours.

Case 3 dwelling is inhabited by a single professional whose work schedule is 8-18h. She reported that she kept some of the windows partially open for ventilation in the day-time, a common local practice also noted in recent research [57], and leaving the windows open overnight. The general low levels of CO_2 concentration and the indoor RH hourly evolution measured (with indoor and outdoor values running frequently in parallel) confirm this, making it difficult to draw conclusions about the occupancy hours. Therefore, the Case 3 occupancy profile definition was based on the hours of presence stated in the survey. She also reported that she rarely made use of the cooling system, only during heat waves, when the system was used for no more than two hours. The measured data confirmed this: the cooling was switched on (OATs ranging from 38 to 42 ºC) on just 2 days out of 11 and kept running below the set point temperatures of 29-30ºC for just 2 hours (**Fig. 13**c). Case 3 presents the lower power consumption: 1327.4 kWh/year, including 440 kWh for the June-September period, that is, almost half of Case 1, four times less than Case 2 and five times lower than the national

average for the Mediterranean climate mentioned above. Two Case 3 sample days are depicted in **Fig. 16**.

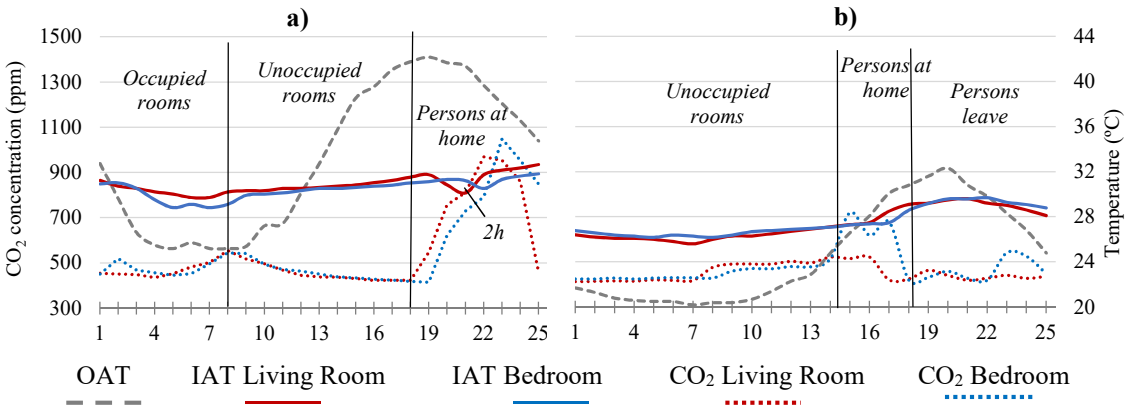

Fig. 16. Case 3. User pattern on two sample days: (a) heat wave and use of cooling system, (b) night-time natural ventilation and no use of the cooling system. Cooling cycle duration is marked on the graphs in hours.

4. Results and discussion

4.1. Indoor environmental evaluation

4.1.1. Indoor air quality, natural ventilation and relative humidity

The hourly evolution of indoor CO_2 concentration and RH registered for the typical periods were analysed (**Table 5**) and depicted in **Fig. 17**. The CO_2 concentration upper limit adopted of 1200 ppm [33] was never exceeded due to the common practice of natural ventilation, the low occupancy and the habit of keeping the interior doors open. IRH remained within the recommended range of 20-70% set in European standard EN15251[34], exceeding it sporadically in Cases 1 and 2; its evolution allowed us to identify the NNVC, as the indoor rates tend to be closer to the outdoor ones (**Fig. 17**). The high thermal inertia of the envelope of Case 1, combined with the moderate use of the cooling system (58% of occupied hours) and the natural night-time ventilation habit and effectiveness prevents the IATs from increasing excessively in both rooms. Although occasional high IRH levels were recorded in the bedroom when it was used for clothes drying, Case 1 showed the greatest IRH stability and independence of ORH conditions. Cases 2 and 3 display similar IAT average values, despite the

marked differences in cooling use. Case 2 IATs were just under 32 ºC on the hottest days (**Fig. 12**b), due to the inherent difficulty of generating cross-ventilation and the resulting limited NNVE, combined with the low thermal inertia of the living room. In short, of the three case studies Case 1 dwelling showed the best indoor thermal conditions. The worst IAT performance was observed in all bedrooms throughout the day, due to the lack of cooling systems.

Table 5
Indoor environmental parameters for the three case studies

Outdoor	**Case 1**		**Case 2**		**Case 3**	
Max OAT (ºC)	40		42			
Min OAT (ºC)	21		19			
Max RH (%)	84		87			
Min RH (%)	21		13			
Indoor	L	B	L	B	L	B
Temperature (ºC)						
Average	28	28	29	30	29	29
Maximum	30	31	33	32	33	32
Minimum	22	24	24	28	25	26
CO_2 concentration (ppm)						
Average	475	476	493	492	436	455
Maximum	852	718	1035	816	970	1049
Relative humidity (%)						
Maximum	67	76	70	62	65	66
Minimum	29	32	19	26	22	25
% occupied hours of cooling use	58%		66%		4%	
Average electricity consumption June-September (kWh)	964		1452		440	
Thermal Stability Coefficient (TSC)	0,11	0,13	0,34	0,12	0,4	0,4
NNVE (ºC per hour)	0,7		0,4		0,5	

L: Living room, B: Bedroom

4.1.2. Thermal comfort

Following the method described in **Section 2.3**, three adaptive comfort models were applied to each case: the MM model [38], Standard 55 from ASHRAE [36] and prEN 16798-1 from CEN [37]. The average deviation of the measured IATs in relation to the daily optimal indoor operative temperature (T_{op}) and the percentage of occupied hours of discomfort were calculated for each model and compared to the percentage of occupied hours of cooling use. The results are summarized in **Tables 1, 2 and 3 of Supplementary Data** and shown in **Fig. 18** and **Fig. 19**.

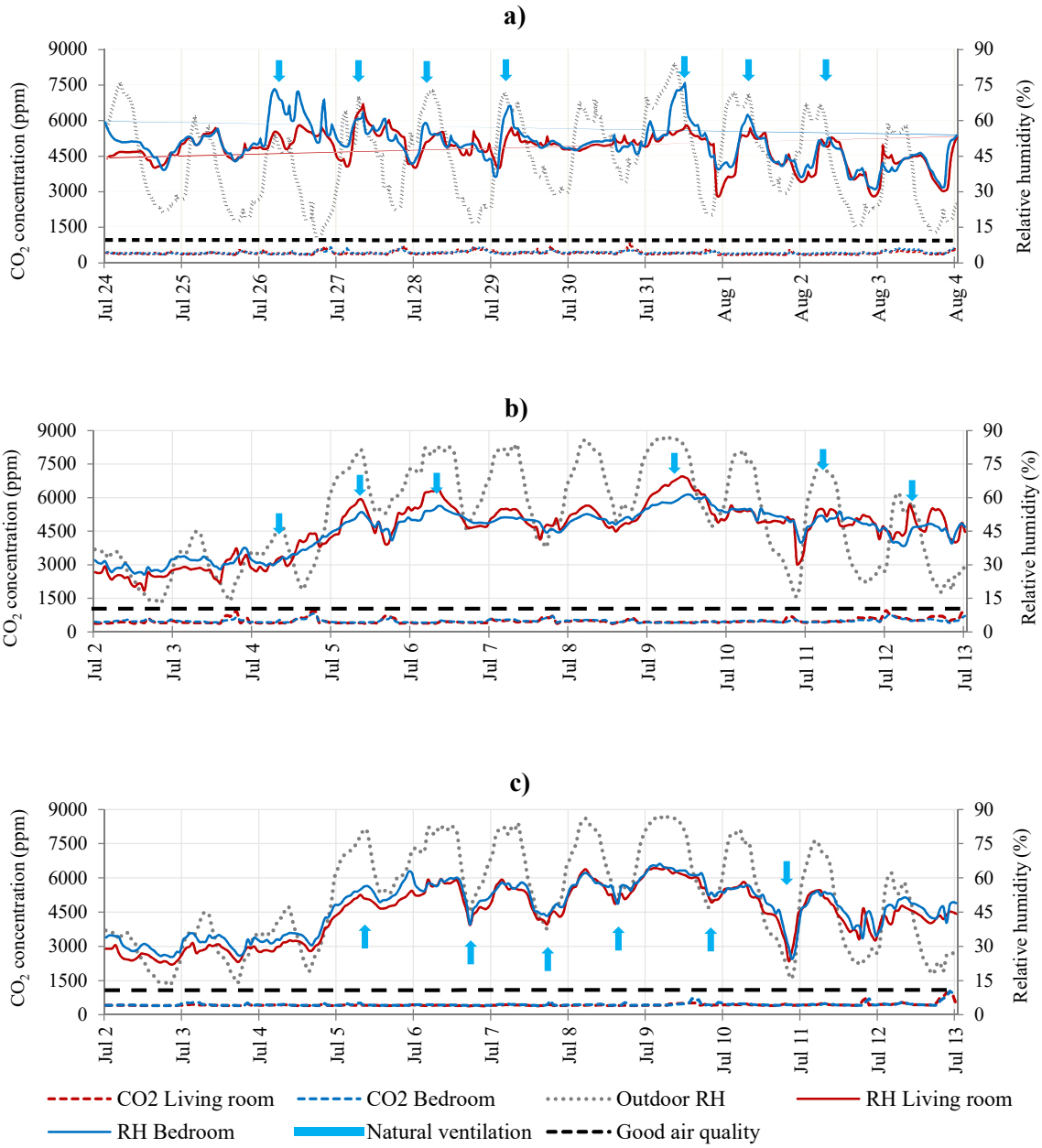

Fig. 17. Hourly evolution of indoor CO_2 concentration and relative humidity in the typical period: (a) Case 1, (b) Case 2, (c) Case 3. The black dashed line indicates the upper limit for good air quality. Natural ventilation periods are represented by blue arrows.

Under the three adaptive models applied, Case 1 shows the best thermal performance: under the most restrictive model (MM), its IAT average deviation in relation to T_{op} is around 2 ºC, while that of Case 2 is near 4 ºC and that of Case 3 is about 3 ºC (average living room and bedroom respectively). The disparity between the MM and Standard 55 models regarding the comfort in Case 1 bedroom is

remarkable. If considering the less restrictive model prEN16798-1, living room and bedroom of Case 1 are almost always in comfort conditions (**Fig. 18**).

Since Case 2 bedroom can barely be refreshed at night, IATs are above 31 ºC during 44% of the total hours, making it the most uncomfortable space of the three case studies, with 100% of discomfort hours under the most restrictive MM model. Its living room shows better thermal quality: under the MM and Standard 55 it was in discomfort for 34% of occupied day-time hours (**Fig. 19**b). Although the cooling was usually set at a conservative temperature, its low efficiency (EER = 2.30) may partially contribute to the electric consumption of this dwelling, the highest of the three case studies. The regular overnight natural ventilation of Case 2 living room did not always guarantee long-lasting 'natural' thermal comfort or its resulting energy and CO_2 emissions savings.

For half of the day-time occupied hours, the living room in Case 3 was thermally uncomfortable (**Fig. 19**c), while conditions of discomfort occurred during 38% of the night-time hours for the bedroom under the MM model. These values are much lower when the less restrictive model is applied, 20% and 0.0% for the living room and bedroom respectively, highlighting the major discrepancy between both models. Case 3 exhibited a reasonably good thermal performance under the severe summer conditions despite the high U-values of the envelope, reduced compactness (**Table 2** and **Table 3**) and limited use of the mechanical cooling system (4% of occupied hours, see **Table 5**); . Although electricity consumption during summer in Case 3 was a third of that of Case 2, the hours of discomfort in its living room were only 16% higher.

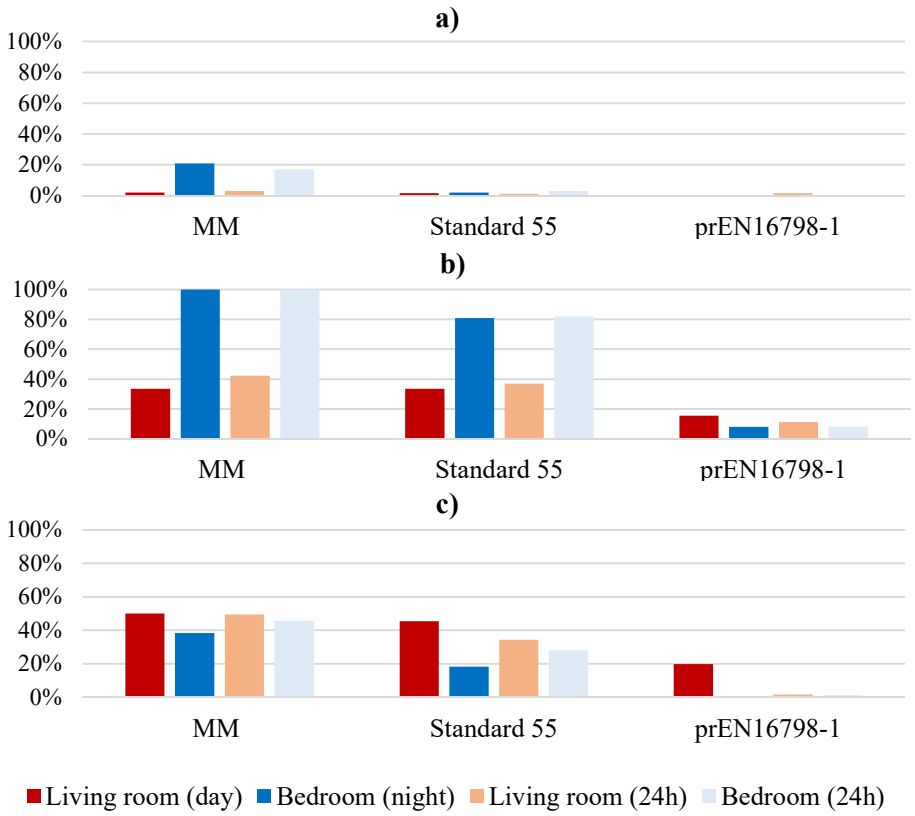

Fig. 18. Percentage of hours of discomfort during the sample period for the three case studies: (a) Case 1, (b) Case 2 and (c) Case 3. Comparison under the three adaptive models and the two occupancy profiles.

The results show that only Case 1 was thermally comfortable for most of the time, with 58% of occupied hours of cooling operation and moderate electricity consumption in summer. The thermal comfort conditions in the other two dwellings were not acceptable. With the exception of Case 3, where living room and bedroom indoor conditions run parallel, the bedrooms were significantly less comfortable than the living rooms during the period analysed. This was partly due to the absence of mechanical cooling systems which led to a reliance on night-time natural ventilation for thermal comfort. According to the analysis featured in **Section 4.1.1.**. this passive strategy alone may be not enough to maintain comfortable sleeping IATs.

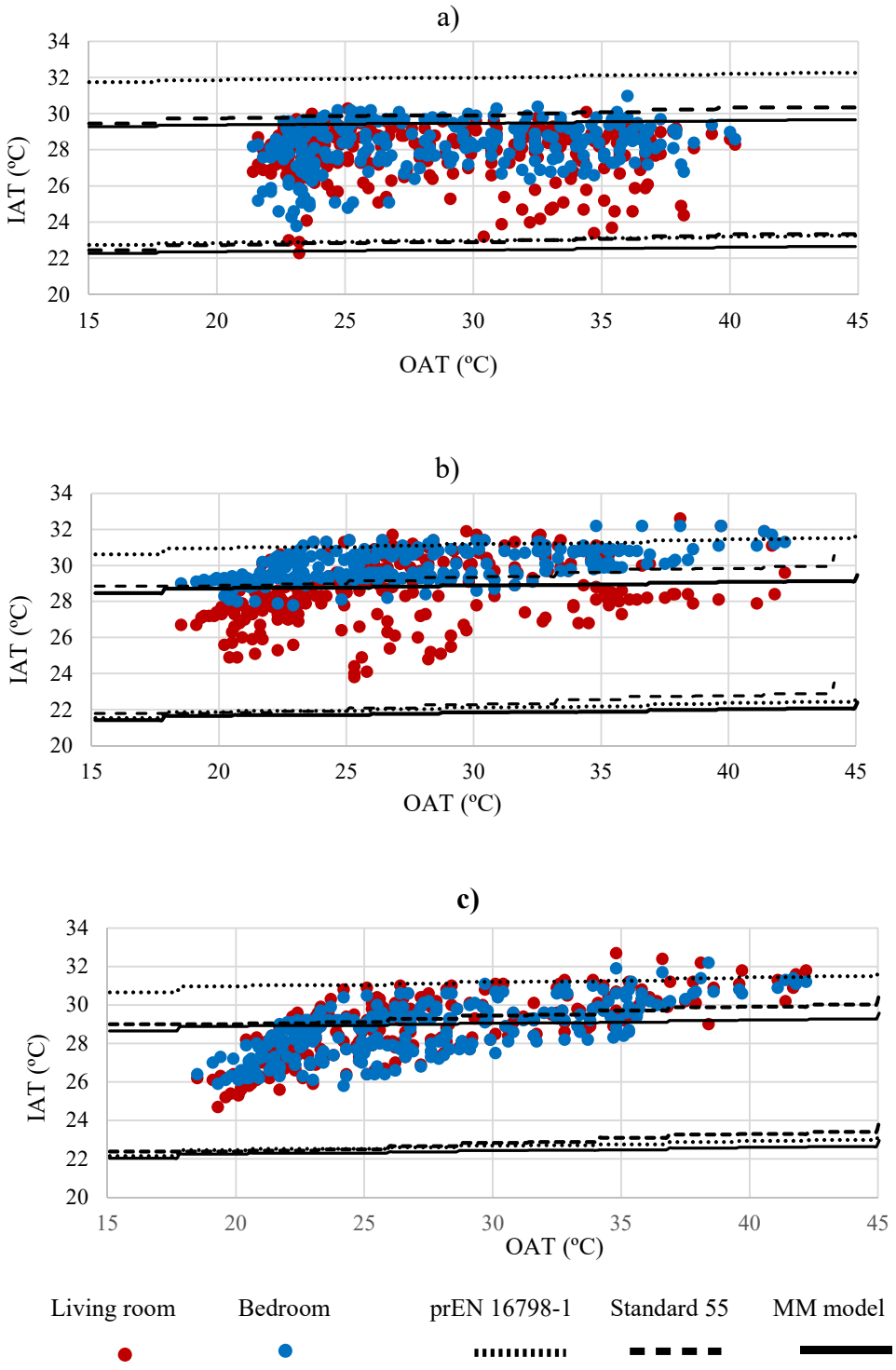

Fig. 19. Thermal comfort evaluation during the sample period for the three case studies: (a) Case 1, (b) Case 2 and (c) Case 3. Comparison under the three adaptive models.

4.2. Energy assessment

4.2.1. Energy model validation

The three energy models were constructed following the method described in **Section 2.4.** This was followed by the graphic comparison of the hourly IAT values obtained in the energy simulations for the typical week of each case and the corresponding hourly IAT values measured during the monitoring campaign. The parameters with higher levels of uncertainty, such as air changes per hour during natural ventilation cycles, window shutter operation and occupants' metabolic rates, were iteratively adjusted in the model until both graphs met approximately as shown in **Fig. 20**A measurement error of ±0.5ºC was considered. Two statistical indexes, Mean Bias Error (MBE) and Coefficient of variation of the Root Mean Square Error (CvRMSE), were calculated afterwards for the data pair for each case study, following the U.S. Department of Energy M&V Guidelines [45]. The results summarized in **Table 6** show the good adjustment achieved.

Table 6
Statistical validation of the energy models (temperature measured in degrees Celsius).

	MBE		CvRMSE	
	Living room	*Bedroom*	*Living room*	*Bedroom*
Case 1	-0.1%	0.2%	2.2%	2.4%
Case 2	-0.5%	0.0%	1.9%	0.6%
Case 3	-0.4%	-0.4%	2.0%	1.7%
ASHRAE Guideline Limit	<10%		<30%	

4.2.2. Energy balance and potential for CO_2 emissions reduction

The energy parameters were organized into two groups, the first of which includes the user-driven thermal loads and the second the building-driven ones, which are strictly dependent on the physical condition of the envelope. Table 4 from the Supplementary section shows these grouped thermal loads, considering the average living room and bedroom rates during the typical week for the three case studies. **Fig. 21**represents the outputs of the calibrated models in bar charts.

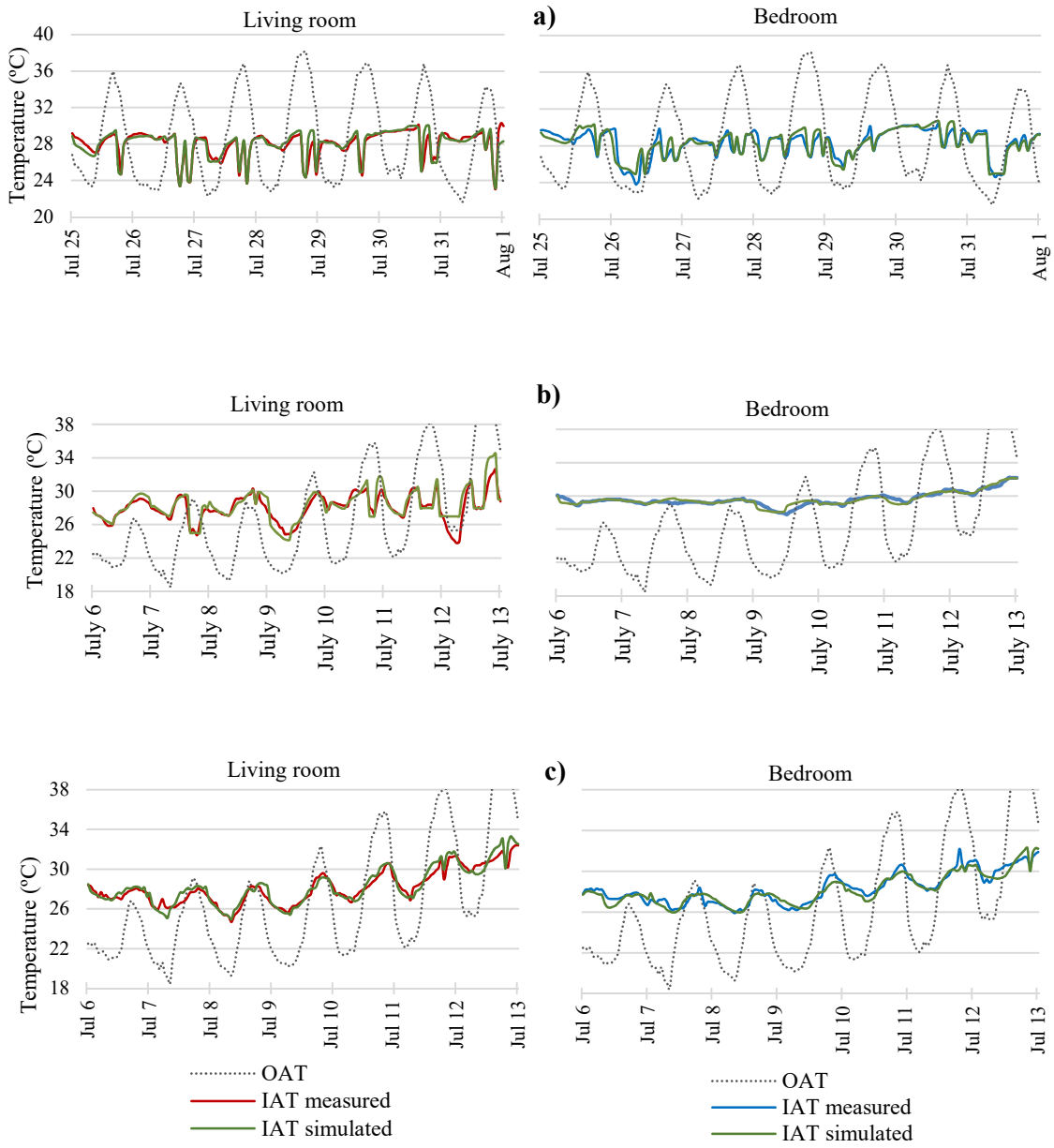

Fig. 20. Graphic calibration of the energy models: (a) Case 1, (b) Case 2, (c) Case 3.

According to the calibrated models, and extrapolating the typical week performance to the whole summer, cooling demand for Cases 1 and 2 were close to the reference national value of 23.4 kWh/m^2 per year for climate zone B4 [58], while that for Case 3 was extremely low (0.5 kWh/m^2 per year) since it was rarely mechanically cooled. Despite demanding the same energy for cooling, the percentage of discomfort hours of Case 2 is more than 6 times greater than that for Case 1 (**Section 4.1.2**) and its electric consumption is 1.50 times higher (**Section 3.3.3**).

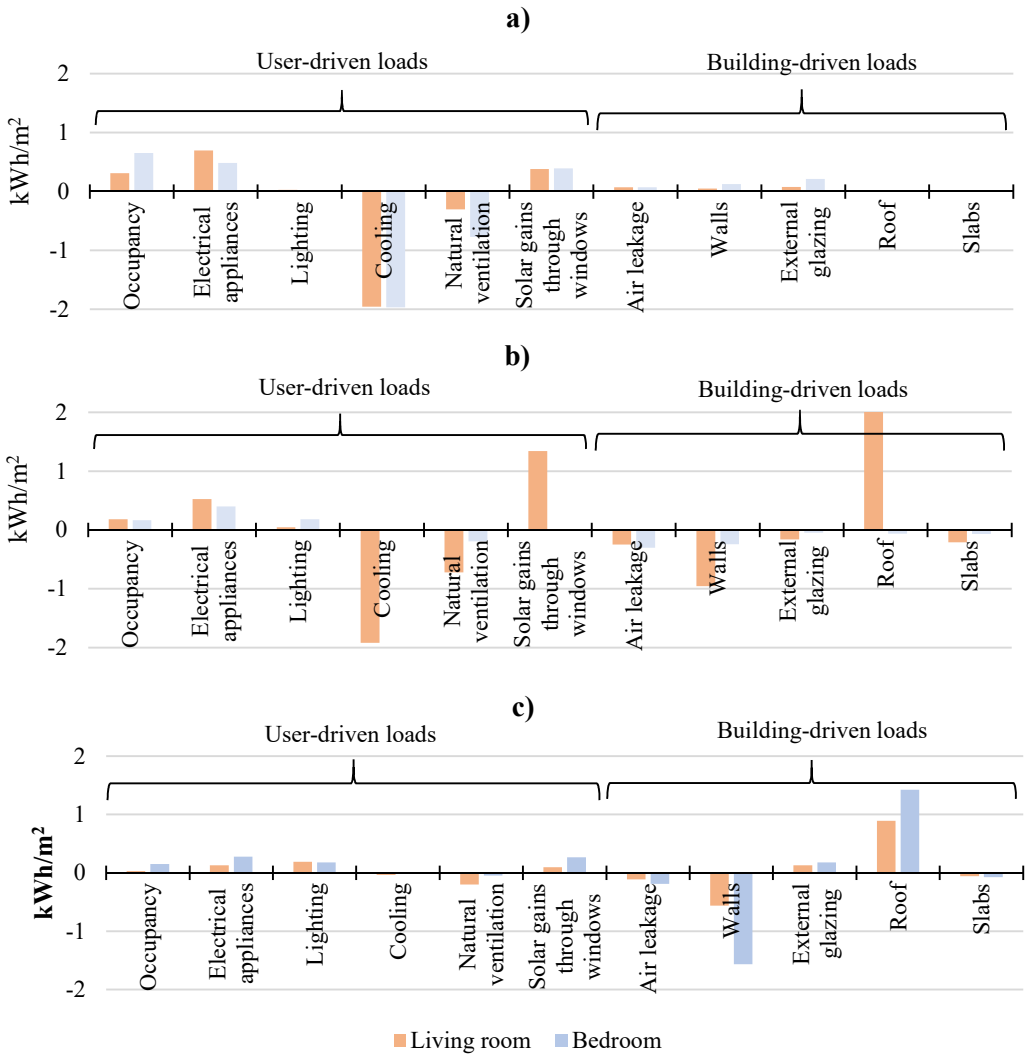

Fig. 21. Heat gains and losses for living room and bedroom during the typical week, referring to usable surface for Case 1 (a), Case 2 (b) and Case 3 (c). Note that for Case 2 (b) bedroom, 'Glazing' refers to internal glazing and 'Roof' refers to upper slab. User-driven and building-driven heat gains/losses have been grouped.

The heat flow balance was negative for Cases 1 and 2 with values around -0.3 kWh/m^2 due to the regular cooling use and natural night ventilation habits reported in **Section 4.1.1.** for both cases. However, most of the thermal loads of Case 1 are user-driven (86%), while those of Case 2 were user and building-driven in equal parts. Case 3 is the only case in which the heat gains exceeded the heat losses with a nearly zero balance (0.14 kWh/m^2). Most of its thermal loads were building-driven (80%) while user-driven loads accounted for only 20% of the total. Its low occupancy, the infrequent use of the cooling system, and the slight refreshment derived from natural ventilation explain this.

The good performance of Case 1 is caused by its high compactness index and thermal mass which barely allowed heat flow (see **Table 3** and **Table 5**). However, as shown in **Fig. 21**a, this, combined with the air leakage through the envelope, had a slightly detrimental effect. External glazing and solar radiation through the windows added 7% and 19% of the total heat gains respectively. Favourable heat loss was entirely user-driven and caused by a combination of strategies: one active, the cooling operation (79%), and another passive, the natural night-time ventilation (21%).

Most of the adverse heat-gains in the living room of Case 2 (**Fig. 21**b) came through the roof and through the window due to the solar radiation. The favourable heat loss for Case 2 was derived from cooling (34%), natural ventilation (17%) and envelope outflows (49%). The last was caused by a combination of three factors: the flow through walls, the air leakage and the glazing of the living room. Due to its east-facing façade, this external glazing was responsible for a favourable 3.5% of Case 2 total heat losses.

As shown in **Fig. 21**c, the heat gains of Case 3 were derived mostly from the roof (60%) and the glazing (8%). It showed the lowest solar gains through the windows, in accordance with the suitable operation of the window shutters recorded during the calibration process. Natural ventilation caused a modest cooling effect, just 7% of total heat loss; while the wall outflows accounted for the largest part.. The low compactness and high thermal transmittance of the walls of Case 3 (see **Table 3** and **Table 5**) made a positive contribution to the summer energy balance.

All of the above indicate that in order to approximate the three case-study performance to the CTE-HE [55] thresholds for cooling demand, primary energy consumption and CO_2 emissions for the summer season, the following measures should be implemented:

- Increase in the natural night-time ventilation efficiency, for Case 3.
- Ensuring an effective window shading, for Cases 1 and 2.
- Glazing enhancement, for Cases 1 and 3 (South facing façades)

- Insulation of the roof, for Cases 2 and 3.

In conclusion, the high thermal transmittance of the roof in Cases 2 and 3 is the only energy parameter dependent on the building envelope and with a clear unfavourable impact in summer. Extensive previous research on housing energy performance in the same climate zone [20], [59] shows that roofs also cause major heat losses during winter and require thermal insulation. Other constructive deficiencies, such as high thermal transmittance of walls and glazing and air leakage, might be beneficial under extreme summer conditions and their transformation would need further consideration.

5. Conclusions

In this paper, we have carried out a triple evaluation of dwellings in representative listed buildings of the historic city of Seville under summer conditions: indoor environmental quality, adaptive thermal comfort and energy performance. Four main conclusions are drawn:

1. Climate change mitigation emerges as a key topic in energy efficiency in historic buildings: the dwellings analysed cause more CO_2 emissions than recently constructed buildings, despite their low energy consumption, because the energy is entirely supplied from the public electricity grid. According to our results, although passive strategies can help mitigate the extreme summer outdoor temperatures, comfortable indoor environment conditioning in urban areas should not rely exclusively on these and would require active cooling system operation in most cases and especially during sleep. Consequently, in order to bring CO_2 emissions down to current standards and guarantee reasonable thermal comfort in historic housing it will be necessary to improve cooling efficiency, implementing mixed energy systems using both renewable and non-renewable energy sources.
2. Any sustainable energy retrofit plan for heritage housing should include occupants' summer thermal comfort, as indoor heat stress is linked to adverse health effects and the increased

mortality risks [60]–[63]. The disparities observed between the three adaptive comfort standards applied call for a better understanding of how comfort conditions are actually pursued in the particular context of older Mediterranean cities, where the hybrid operation of buildings, alternating natural and mechanical cooling [38], is widely practiced.

3. The user-driven thermal loads on domestic spaces in historic buildings has a significant effect on the overall energy demand. The diversity observed in residents' practices suggests that standardized user patterns are not suited to energy assessment in historic buildings, as has been shown to be the case for social housing [13], [23], [57] because they may induce the unintended pre-bound effect after intervention [64].
4. Reducing the mechanical cooling demand of the dwellings and making most of them produce less pollution would not require intrusive physical transformations. Other non-intrusive, inexpensive and technically feasible measures, in line with their heritage assets preservation, would suffice. As shown in **Section 4.2.2.** except for the top floor dwellings, the energy balance optimization under summer conditions would largely consist of suitable window shading fitting and operation, as well as of appropriate use of night-time natural ventilation, when outdoor conditions allow.

BIBLIOGRAPHY

[1] United Nations, “Sustainable Development Goals. Press materials (3 april 2017).” [Online]. Available: https://www.un.org/sustainabledevelopment/blog/2017/04/more-action-needed-to-meet-energy-goals-by-2030-new-report-finds/. [Accessed: 18-Feb-2019].

[2] A. L. Webb, “Energy retrofits in historic and traditional buildings: A review of problems and methods,” *Renew. Sustain. Energy Rev.*, vol. 77, no. April 2016, pp. 748–759, 2017.

[3] UNESCO, “Recommendation on the Historic Urban Landscape,” 2011.

[4] ICOMOS, “The Valletta Principles for the Safeguarding and Management of Historic Cities, Towns and Urban Areas,” 2011.

[5] R. Caro-Martínez and J. J. Sendra, “Implementation of urban building energy modeling in historic districts. Seville as case-study,” *Int. J. Sustain. Dev. Plan.*, vol. 13, no. 4, 2018.

[6] EU Seventh Framework Programme., “Climate for Culture,” *2009-2014*. [Online]. Available: https://www.climateforculture.eu/. [Accessed: 11-Mar-2019].

[7] EU Intelligent Energy Europe Programme, “3encult. Efficient energy for EU cultural heritage,” *2010-2014*. [Online]. Available: http://www.3encult.eu/en/project/welcome/default.html. [Accessed: 11-Mar-2019].

[8] EU Seventh Framework Programme, “EFFESSUS. Energy Efficiency for EU Historic Districts’ Sustainability,” *2012-2016*. [Online]. Available: http://www.effesus.eu/. [Accessed: 11-Mar-2019].

[9] A. Martínez-Molina, I. Tort-Ausina, S. Cho, and J. L. Vivancos, “Energy efficiency and thermal comfort in historic buildings: A review,” *Renew. Sustain. Energy Rev.*, vol. 61, pp. 70–85, 2016.

[10] S. Lidelöw, T. Örn, A. Luciani, and A. Rizzo, “Energy-efficiency measures for heritage buildings: A literature review,” *Sustain. Cities Soc.*, vol. 45, no. June 2018, pp. 231–242, 2018.

[11] F. Berg, A.-C. Flyen, Å. Lund Godbolt, and T. Broström, “User-driven energy efficiency in historic buildings: A review,” *J. Cult. Herit.*, vol. 28, pp. 188–195, 2017.

[12] L. Tjørring and Q. Gausset, “Drivers for retrofit: a sociocultural approach to houses and inhabitants,” *Build. Res. Inf.*, vol. 47, no. 4, pp. 394–403, 2019.

[13] O. Guerra-Santin, “Relationship Between Building Technologies, Energy Performance and Occupancy in Domestic Buildings,” in *Living Labs*, D. Keyson, O. Guerra-Santin, and D. Lockton, Eds. Springer, Cham, 2017, p. 396.

[14] A. Monge-Barrio and A. Sánchez-Ostiz Gutiérrez, “Facing Heatwaves and Warming Conditions in the Mediterranean Region,” in *Passive energy strategies for Mediterranean residential buildings*, 2018, p. 38.

[15] G. Ciulla, A. Galatioto, and R. Ricciu, “Energy and economic analysis and feasibility of retrofit actions in Italian residential historical buildings,” *Energy Build.*, vol. 128, pp. 649–659, Sep. 2016.

[16] A. Galatioto, G. Ciulla, and R. Ricciu, “An overview of energy retrofit actions feasibility on Italian historical buildings,” *Energy*, vol. 137, pp. 991–1000, Oct. 2017.

[17] L. De Santoli, “Reprint of: ‘Guidelines on energy efficiency of cultural heritage,’” *Energy Build.*, vol. 95, pp. 2–8, 2015.

[18] M. De Fino, A. Scioti, E. Cantatore, and F. Fatiguso, “Methodological framework for assessment of energy behavior of historic towns in Mediterranean climate,” *Energy Build.*, vol. 144, pp. 87–103, 2017.

[19] A. Perez-Garcia, A. P. Guardiola, F. Gómez-Martínez, and A. Guardiola-Víllora, “Energy-saving

potential of large housing stocks of listed buildings, case study: l'Eixample of Valencia," *Sustain. Cities Soc.*, vol. 42, pp. 59–81, Oct. 2018.

[20] J. J. Sendra, *Proyecto Efficacia : optimización energética en la vivienda colectiva*. Sevilla: Secretariado de Publicaciones de la Universidad de Sevilla, 2011.

[21] J. J. Sendra, S. Domínguez-Amarillo, P. Bustamante, and a. L. León, "Energy intervention in the residential sector in the south of Spain: Current challenges," *Inf. la Construcción*, vol. 65, no. 532, pp. 457–464, 2014.

[22] R. Escandón, R. Suárez, and J. J. Sendra, "On the assessment of the energy performance and environmental behaviour of social housing stock for the adjustment between simulated and measured data: The case of mild winters in the Mediterranean climate of southern Europe," *Energy Build.*, vol. 152, pp. 418–433, 2017.

[23] R. Escandón, R. Suárez, and J. J. Sendra, "Field assessment of thermal comfort conditions and energy performance of social housing: The case of hot summers in the Mediterranean climate," *Energy Policy*, vol. 128, no. July 2018, pp. 377–392, 2019.

[24] N. Ramos *et al.*, "Indoor hygrothermal conditions and quality of life in social housing : A comparison between two neighbourhoods," *Sustain. Cities Soc.*, vol. 38, no. December 2017, pp. 80–90, 2018.

[25] A. Curado and V. P. De Freitas, "Influence of Thermal Insulation of Facades on the Performance of Retrofitted Social Housing Buildings in Southern European Countries," *Sustain. Cities Soc.*, 2019.

[26] R. Escandón, R. Suárez, and J. José Sendra, "Protocol for the energy behaviour assessment of social housing stock: the case of southern Europe," *Energy Procedia*, vol. 96, pp. 907–915, 2016.

[27] T. Blázquez, R. Suárez, and J. J. Sendra, "Towards a calibration of building energy models: A case study from the Spanish housing stock in the Mediterranean climate," *Inf. la Construcción*, vol. 67, no. 540, p. e128, Dec. 2015.

[28] J. Fernández-Agüera, S. Domínguez-Amarillo, J. J. Sendra, and R. Suárez, "An approach to modelling envelope airtightness in multi-family social housing in Mediterranean Europe based on the situation in Spain," *Energy Build.*, vol. 128, pp. 236–253, 2016.

[29] S. Domínguez-Amarillo, J. Fernández-Aguera, and M. Á. Campano, "Effect of Airtightness on Thermal Loads in Legacy Low-Income Housing," no. Equation 1, pp. 1–15, 2019.

[30] *Thermal performance of buildings. Determination of air permeability of buildings. Fan pressurization method. UNE EN 13829.* 2013.

[31] Gobierno de España, "AEMET (Agencia Estatal de Meteorología)." [Online]. Available: http://www.aemet.es/es/portada. [Accessed: 10-Feb-2019].

[32] J. Neila González, *Arquitectura bioclimática : en un entorno sostenible*. Munillalería, 2004.

[33] Finnish Society for Indoor Air Quality and Climate FiSIAQ, *Finnish Classification of Indoor Environment. Taget values, design guidance and products requirements.* 2008.

[34] CEN/TC 156, *Indoor environmental input parameters for design and assessment of energy performance of buildings addressing indoor air quality, thermal environment, lighting and acoustics (prEN15251-1:2007)*. European Union, 2007, p. 48.

[35] S. Carlucci, L. Bai, R. de Dear, and L. Yang, "Review of adaptive thermal comfort models in built environmental regulatory documents," *Build. Environ.*, vol. 137, no. March, pp. 73–89, 2018.

[36] ASHRAE, *Thermal environmental conditions for human occupancy. Standard 55-2017*. 2017.

[37] CEN/TC 156, *Indoor environmental input parameters for design and assessment of energy performance of buildings addressing indoor air quality, thermal environment, lighting and acoustics.*

Module M1-6 (prEN 16798-1:2015), vol. 44, no. 0. 2015.

[38] E. Barbadilla-Martín, J. M. Salmerón Lissén, J. Guadix Martín, P. Aparicio-Ruiz, and L. Brotas, "Field study on adaptive thermal comfort in mixed mode office buildings in southwestern area of Spain," *Build. Environ.*, vol. 123, pp. 163–175, 2017.

[39] Ministerio de Fomento del Gobierno de España, *Código Técnico de la Edificación. Documento Básico HE de Ahorro de Energía*. 2017, pp. 1–129.

[40] J. Cipriano, G. Mor, D. Chemisana, D. Pérez, G. Gamboa, and X. Cipriano, "Evaluation of a multi-stage guided search approach for the calibration of building energy simulation models," *Energy Build.*, vol. 87, pp. 370–385, 2015.

[41] T. A. Reddy, "Literature review on calibration of building energy simulation programs: uses, problems, procedures, uncertainty, and tools," *ASHRAE Trans.*, vol. 112, no. Part I, pp. 226–240, 2006.

[42] ASHRAE, "Measurement of Energy , Demand , and Water Savings. Guideline 14-2014.," 2014.

[43] U.S. Department of Energy, "Energy Plus." [Online]. Available: https://energyplus.net/. [Accessed: 10-Feb-2019].

[44] DOE, "U.S. Department of Energy." [Online]. Available: https://www.energy.gov/. [Accessed: 10-Apr-2019].

[45] U.S. Department of energy, *M & V Guidelines : Measurement and Verification for Performance-Based Contracts Version 4.0.*, no. November. 2015, p. 108.

[46] UNESCO. World Heritage Convention, "World Heritage Centre." [Online]. Available: https://whc.unesco.org/en/list/383. [Accessed: 02-Apr-2019].

[47] Gerencia de Urbanismo del Ayuntamiento de Sevilla, "Infraestructura de datos espaciales de Sevilla (ide.SEVILLA)." [Online]. Available: https://sig.urbanismosevilla.org/InicioIDE.aspx. [Accessed: 11-Feb-2019].

[48] M. Kottek, J. Grieser, C. Beck, B. Rudolf, and F. Rubel, "World map of the Köppen-Geiger climate classification updated," *Meteorol. Zeitschrift*, vol. 15, no. 3, pp. 259–263, 2006.

[49] "Agencia Andaluza de la Energía." [Online]. Available: https://www.agenciaandaluzadelaenergia.es/Radiacion/radiacion3.php. [Accessed: 11-Feb-2019].

[50] C. M. Calama-González, R. Suárez, Á. L. León-Rodríguez, and S. Domínguez-Amarillo, "Evaluation of thermal comfort conditions in retrofitted facades using test cells and considering overheating scenarios in a mediterranean climate," *Energies*, vol. 11, no. 4, 2018.

[51] A. Villar Movellán, *Arquitecto Espiau (1879-1938)*. Diputación Provincial de Sevilla, 1985.

[52] F. Pérez Gálvez, "Las obras de fábrica en la arquitectura doméstica sevillana de los siglos XVIII y XIX. Características constructivas y parámetros resistentes.," University of Seville, 2004.

[53] A. González Cordón, "Sevilla 1849-1929. Arquitectura y ciudad. La vivienda obrera y lo urbano en la formación de la ciudad contemporánea," University of Seville, Spain, 1981.

[54] J. Fernández-Agüera, S. Domínguez-Amarillo, J. J. Sendra, R. Suárez, and I. Oteiza, "Social housing airtightness in Southern Europe," *Energy Build.*, vol. 183, pp. 377–391, 2018.

[55] Ministerio de Fomento del Gobierno de España, *Código Técnico de la Edificación. Docuemnto básico de ahorro de energía (CTE-DB-HE)*. 2017.

[56] E. Y. T. E. IDAE, Instituto para la diversificación y Ahorro de la Energía. Ministerio de industria, "Consumos del sector residencial en España Resumen de Información Básica," 2016.

[57] S. Domínguez-Amarillo *et al.*, "Rethinking User Behaviour Comfort Patterns in the South of Spain—

What Users Really Do," *Sustainability*, vol. 10, no. 12, p. 4448, 2018.

[58] G. de T. de la E. S. de I. I. de la U. de S. AICIA, "Condiciones de aceptación de procedimientos alternativos a LIDER y CALENER. Anexos." IDAE y Ministerio de La Vivienda, 2009.

[59] S. Domínguez Amarillo, "Building envelopes and social housing in southern Europe energy assessment of the residential social stock of the city of Seville under the climate change scenario," University of Seville, Spain, 2016.

[60] J. Díaz *et al.*, "Heat waves in Madrid 1986–1997: effects on the health of the elderly," *Int. Arch. Occup. Environ. Health*, vol. 75, no. 3, pp. 163–170, Mar. 2002.

[61] R. S. Kovats and S. Hajat, "Heat Stress and Public Health: A Critical Review," *Rev. Adv. Annu. Rev. Public Heal.*, vol. 29, pp. 41–55, 2008.

[62] J. Paravantis, M. Santamouris, C. Cartalis, C. Efthymiou, and N. Kontoulis, "Mortality Associated with High Ambient Temperatures, Heatwaves, and the Urban Heat Island in Athens, Greece," *Sustainability*, vol. 9, no. 4, p. 606, Apr. 2017.

[63] A. Pyrgou and M. Santamouris, "Increasing Probability of Heat-Related Mortality in a Mediterranean City Due to Urban Warming," *Int. J. Environ. Res. Public Health*, vol. 15, no. 8, p. 1571, 2018.

[64] M. Sunikka-Blank and R. Galvin, "Introducing the prebound effect: the gap between performance and actual energy consumption," *Build. Res. Inf.*, vol. 40, no. 3, pp. 260–273, Jun. 2012.